Date of publication JUN-28, 2021, date of current version JUN-02, 2021.
www.computingonline.net / computing@computingonline.net

Print ISSN 1727-6209
Online ISSN 2312-5381
DOI 10.47839/ijc.20.2.2069

New Hypertensive Retinopathy Grading Based on the Ratio of Artery Venous Diameter from Retinal Image

BAMBANG KRISMONO TRIWIJOYO[1,2], BOY SUBIROSA SABARGUNA[3], WIDODO BUDIHARTO[1], EDI ABDURACHMAN[1]

[1]Binus Graduate Program Bina Nusantara University, Jl. Kebon Jeruk No.27, Jakarta, Indonesia
(e-mail: bambang.triwijoyo@binus.ac.id, wbudiharto@binus.edu, edia@binus.edu)
[2]Department of Computer Science, Faculty of Engineering and Health, Bumigora University, Jl. Ismail Marzuki, Mataram, West Nusa Tenggara, Indonesia (e-mail: bambang.triwijoyo@binus.ac.id)
[3]Department of Community Medicine, Faculty of Medicine, University of Indonesia, Jl. Pegangsaan Timur, Central Jakarta City, Indonesia
(e-mail: sabarguna08@ui.ac.id)

Corresponding author: Bambang Krismono Triwijoyo (e-mail: bambang.triwijoyo@binus.ac.id).

ABSTRACT Medical research indicated that narrowing of the retinal blood vessels might be an early indicator of cardiovascular diseases; one of them is hypertensive retinopathy. This paper proposed the new staging method of hypertensive retinopathy by measure the ratio of diameter artery and vein (AVR). The dataset used in this research is the public Messidor color fundus image dataset. The proposed method consists of image resizing using bicubic interpolation, optic disk detection, a region of interest computation, vessel diameter measuring, AVR calculation, and grading the new categories of Hypertensive Retinopathy based on Keith-Wagener-Barker categories. The experiments show that the proposed method can determine the stage of hypertensive retinopathy into new categories.

KEYWORDS hypertensive retinopathy; grading; artery-vein diameter ratio.

I. INTRODUCTION

CARDIOVASCULAR disease, such as stroke and coronary heart disease, is a major cause of morbidity and mortality worldwide [1]. Studies show that the first major marker of cardiovascular risk is narrowing of the retinal arteries [2]. The measurement that has been used to measure the degree of narrowing is the ratio of arterial-venous diameter (AVR) [3]. The AVR ratio is determined by measuring the diameter of the individual retinal arteries and venous caliber. Lower AVR is associated with higher blood pressure and an increased risk of stroke, diabetes, and hypertension. AVR is calculated by measuring the diameter of the retinal vessels from retinal images; this method requires time and is very operator-dependent. First must be determined the type of vessels (arteries or veins), then measured the diameter of each blood vessel, and then measured manually. This process not only takes time but varies from one inspection to the next, even when the same human being is involved. Therefore, reproducibility is a major concern [4]. The average human grader usually needs to spend up to twenty minutes per retinal image to complete measurements, so this method is certainly not feasible for large-scale research studies and clinical utility. There is a need for a more precise and efficient system that can assess retinal blood vessels automatically. This paper proposes a new method of measuring the ratio of arterial and venous diameter (AVR) and determining the grade of hypertensive retinopathy based on the new category.

Existing techniques for vessel detection in retinal images are classified into two categories: scanning methods [5] and tracking methods [6]. The scanning method requires two-step processing of each pixel image: increase and threshold. Additional tracking steps are needed if the application requires that the vessel structure be identified. Instead, the

tracking approach uses local image properties to track vessels from the starting point. This approach is faster because it only processes pixels that are close to the vessel. In boundary detection, vessel edges are detected by edge detectors [7], morphological methods [8], or deformable models [9]. Mounting edges that minimize the distance between the original data and the predetermined model are used in vessel extraction [5, 10]. It was stronger because it extracted the vessel as a whole.

Various models have been designed to create vascular profiles: regular [11], triangular [12], Elliptical [13], and Gaussian [5, 14]. However, all of these models do not consider the reflection of central light on the vessel [15]. AVR estimation is a challenging task and requires the detection of optical disks in segmented blood vessels. Optical disk detection is needed to determine the area of interest (ROI) when measuring the ship. The semi-automatic method using wavelet Gabor and morphological operations was proposed by Ortiz et al. [16]. This method was tested on a clinically obtained database of 30 images with an accuracy of 57%. Agurto et al. [17] presented the method of ship segmentation based on the improvement of multi-scale linear structures and the second-order local entropy thresholding. This method was tested on 74 fundus images with 80% accuracy. AVR calculations are performed on (0.5-1) optical disk (DD) diameters which can give inappropriate results. Manikis et al. [18] presented the jute-based vessel segmentation method along with thresholds and reached an accuracy of 93.71% and 93.18% for DRIVE and STARE respectively. In the calculation of AVR, the area of interest (ROI) is highly dependent on optical disk detection but they do not provide a clear idea of the optical disk detection method used in their work. Khitran et al. [19] presented a new method of AVR calculation. They tested their method on 58 fundus images from VICAVR and 40 images from the DRIVE database and achieved an accuracy of 96.5% and 98%, respectively. The limitation of their work is that sufficient descriptions of their results are not presented by them. The remainder of this paper is divided into four parts after this introductory part, the material and method sections. Then, the third part discusses the method and results and discussion. In the last section, we conclude the results of this study.

II. MATERIAL AND METHODS

A. THE PROPOSED METHOD

The stages of the proposed method, in general, are summarized in Fig. 1. The main processes are image resizing, optic disk detection, a region of interest computation, vessel diameter measuring, scoring, and labeling.

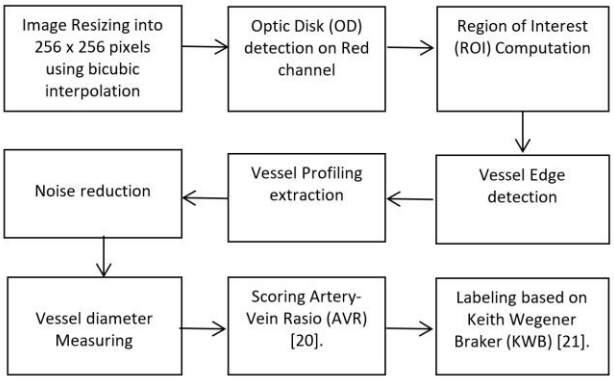

Figure 1. The Stages of the proposed method

B. DATASET

We use secondary data of retinal image dataset from open source database Messidor. This database was consisting of 1200 retinal images of 1440 x 960 pixels in TIFF format downloaded on the page http://www.adcis.net/en/Download-Third-Party/Messidor.html [22]. In this study, we sampled 100 images from the Messidor database in the "Base11" folder, and resized them into image sizes 256 x 256 pixels, respectively using bi-cubic interpolation [23]. Fig. 2 shows a color retinal image showing artery-vein of the blood vessel and optic disk area.

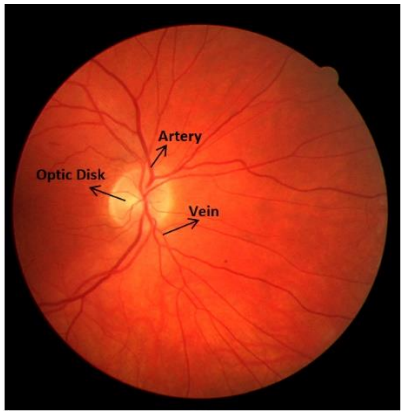

Figure 2. The retinal image

C. RESIZING IMAGE

The input image is resized to 256 x 256 using the bicubic interpolation method [24]. This method was chosen because the result is finer at the edges than the bilinear interpolation. Bi-cubic uses 4 x 4 pixels neighbors to retrieve information. Bicubic produces sharper images and maybe an ideal combination of quality process and output time. To analyze the results of the resizing process, three parameters such as the Mean Square Error (MSE), Root Mean Squared Error (RMSE), and Peak Signal-to-Noise Ratio (PSNR) were used to measure the similarity between two images [25]. These parameters are used to compare the results of resizing the image with the initial image or original image. MSE and

RMSE do not have unit values, while PSNR have decibels (dB) as a unit value, more similar of the two images, then MSE and RMSE values are getting closer to zero. Whereas in PSNR, two images have a low level of similarity if the PSNR value is below 30 dB. The equation used to calculate the three parameters is as follows:

$$MSE = \frac{1}{m \times n} \sum_{i=0}^{n-1} \sum_{j=0}^{m-1} [f(i,j) - g(i,j)]^2 , \quad (1)$$

$$RMSE = \sqrt{MSE}, \quad (2)$$

$$PSNR = 10\ log_{10} \frac{255^2}{MSE}, \quad (3)$$

where *m* is the image height, *n* is the image width, *f(i, j)* is the original image, and *g(i, j)* is the resizing image. To measure the results of resizing, using the bicubic interpolation method, we used 20 sample images and calculated the values of MSE, RMSE, and PSNR, and compared them with two other methods of resizing bilinear interpolation and nearest-neighbor interpolation.

D. OPTIC DISK (OD) DETECTION

Read the red channel of the input image and calculate the average of 1.5 area of OD. Perform histogram analysis for threshold determination, read the highest intensity value of the image, read the number of pixel intensity, read value as a threshold value (T). Perform image segmentation using a threshold value.

$$g(x,y) = \{^{1\ if\ f(x,y) \geq T}_{0\ otherwise} . \quad (4)$$

For each area, the histogram segmentation results, determine initial coordinate points within the area at random, do region growing on eight neighbors [26]. For each area the segmentation results of the growing region determine the center point of the area from the average of its x-y coordinates circle shape detection using Hough transform. For each edge pixel area:

$$x_i = a + R\cos(\theta), \quad (5)$$

$$y_i = b + R\cos(\theta). \quad (6)$$

Calculate the image gradient:

$$G[f(x,y)] = [G_x, G_y] = \left[\frac{\partial f}{\partial x}, \frac{\partial f}{\partial y}\right]. \quad (7)$$

Finally, select the area closest to the shape of the circle as the OD area.

E. REGION OF INTEREST (ROI)

Read the input image of OD area detection results, read the coordinates of the center point of the OD (x_i, y_i), specify the ROI area.

$$r_d = 1.5\ 8\ r\ . \quad (8)$$

Calculate 4 square corner points around the OD area as follows:

$$a = ((x_i - r_d), (y_i - r_d)), \quad (9)$$

$$b = ((x_i + r_d), (y_i - r_d)), \quad (10)$$

$$c = ((x_i - r_d), (y_i + r_d)), \quad (11)$$

$$d = ((x_i + r_d), (y_i + r_d)). \quad (12)$$

Create a square by making a connecting line point *a* to *b*, *b* to *c*, *c* to *d*, and *d* to *a*.

F. VESSEL EDGE DETECTION

Read the ROI area of the input image. Perform edge detection using the Canny algorithm [27]. Read the green channel of the input image and perform median filtering with a 5x5 pixel filter size [28]. Perform histogram analysis for threshold determination. Read the highest intensity value of the image and read the number of pixel intensity, if the number of pixels less than 10 percent of the total number of pixel image, read the second highest intensity, and so on until the number of pixels is more or equal then 10 percent of the total number of the pixel image. Finally, read the value pixel intensity as the threshold value.

G. VESSEL PROFILING EXTRACTION

Read the ROI area of the input image. Draw a line from the center point of the ROI (x_1, y_1) to the point (x_2, y_2) the far edge toward the edge of the ROI area for angle values (θ) from 0 to 359, For each line, determine the coordinate points of the two sides of the left edge of the vessel (L_x, L_y) and the right edge side of the vessel (R_x, R_y).

$$L_x = y_2 - r * sin\left(\theta + \frac{\pi}{2}\right), \quad (13)$$

$$L_y = x_2 + r * cos\left(\theta + \frac{\pi}{2}\right), \quad (14)$$

$$R_x = y_2 - r * sin\left(\theta + 3 * \frac{\pi}{2}\right), \quad (15)$$

$$R_y = x_2 + r * cos\left(\theta + 3 * \frac{\pi}{2}\right). \quad (16)$$

Fig. 3 shows Mapping the points on the left side (L_x, L_y) and right side (R_x, R_y) of an edge pixel (x_2, y_2).

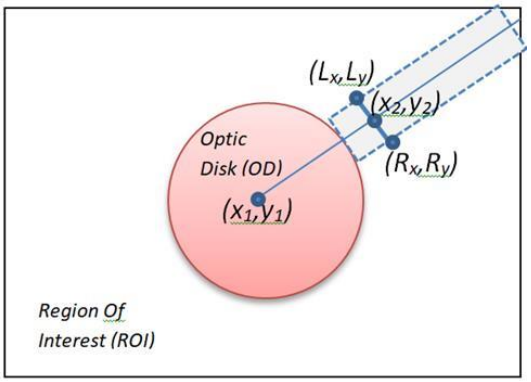

Figure 3. Mapping point (x_1,y_1),(x_2,y_2),(L_x,L_y) and (R_x,R_y)

Read the green channel of the input image, *Do* smoothing Gaussian filter and perform average filtering with 3x3 pixel filter size.

H. NOISE REDUCTION

Read the ROI area of the input image, count the number of edge pixels of each vessel (*N*), read left edge point intensity (*IL*), read right edge pixels intensity (*IR*). If *IL*> *IR* calculate the number of left edge pixels (*NP IL*), else If *IR*> *IL* calculate the number of right edge pixels (*IR NP*). Calculate the ratio of the number of edge pixels. If (*N* / (*NP IL* + *NP IR*)) ≥ 0.95 then the edge of the vessel, else If (*N* / (*NP IL* + *NP IR*)) <0.95 then it is considered noise. Calculate the Euclidian distance of the first edge (x_1, y_1) to the last edge (x_2, y_2):

$$E = \sqrt{(x2 - x1)^2 + (y2 - y1)^2}, \quad (17)$$

if the ratio of (*N* / *E*) ≤ 0.67, then profile is considered not vascular or noise [26].

I. THE VESSEL DIAMETER

Read the ROI area of the input image, For each vessel in the ROI area, (*x*', *y*') is the coordinate of the midpoint on the line of each vessel, *r* is the distance from the center point to the edge of the vessel and θ is rotation angle. For a rotation angle from 0° to 180° to the midpoint (*x*', *y*'), read the first edge point coordinates (x_1, y_1), Read the paired edge position coordinates (x_2, y_2) by adding angles (θ + 180°).

$$x_1 = x' + r * \cos(\theta), \quad (18)$$
$$y_1 = y' + r * sin(\theta). \quad (19)$$

Calculate vessel diameter using Euclidean distance:

$$d = \sqrt{((x_1 - x_2)^2 + (y_1 - y_2)^2)}. \quad (20)$$

Finally, select the minimum d value as the width of the vessel.

J. SCORING OF ARTERY-VEIN RATIO

For the ROI area of each input image, W_a is the widest branch of the smallest artery/vein; W_b is the widest branch of the largest artery/vein. Calculate Central Retinal Artery Equivalent (CRAE):

$$CRAE = \sqrt{(0.87W_a^2 + 1.01W_b^2 - 0.22W_aW_b - 10.73)} \quad (21)$$

Calculate the Central Retinal Vein Equivalent (CRVE):

$$CRVE = \sqrt{(0.72W_a^2 + 0.91W_b^2 + 450.02)}. \quad (22)$$

Calculate Artery-Vein Ratio (AVR) [20].

$$AVR = \frac{CRAE}{CRVE}. \quad (23)$$

K. IMAGE GRADING

For each input image, read the AVR input image and determine the new categories of Retinopathy Hypertension based on Keith-Wagener-Barker categories [21].

If (0.67 ≤ AVR ≤ 0.74) then Normal
If (0.51 ≤ AVR ≤ 0.66) then Borderline 1
If (0.40 ≤ AVR ≤ 0.50) then Grade 1
If (0.34 ≤ AVR ≤ 0.39) then Borderline 2
If (0.31 ≤ AVR ≤ 0.33) then Grade 2
If (0.25 ≤ AVR ≤ 0.30) then Borderline 3
If (0.23 ≤ AVR ≤ 0.24) then Grade 3
If (0.20 ≤ AVR ≤ 0.22) then Borderline 4
If (0.00 ≤ AVR ≤ 0.19) then Grade 4.

III. RESULT AND DISCUSSION

We chose 100 color retinal images from the Messidor dataset and tested them by the proposed method. Firstly, we resized the original retinal image into image-sized 256 x 256 pixels respectively using bi-cubic interpolation. The results of measuring the image in resizing process were obtained using the bicubic interpolation of 20 sample color images, for each color channel Red (R), Green (G), and Blue (B) calculated MSE, RMSE, and PSNR indicators and averages (AVG) for all channels color.

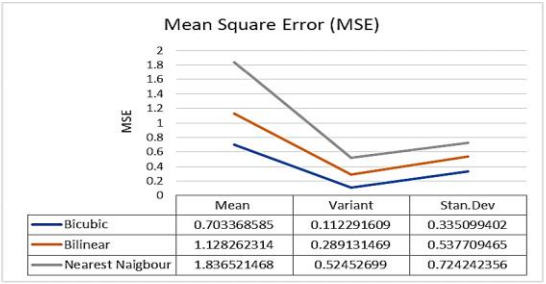

	Mean	Variant	Stan.Dev
Bicubic	0.703368585	0.112291609	0.335099402
Bilinear	1.128262314	0.289131469	0.537709465
Nearest Naigbour	1.836521468	0.52452699	0.724242356

(a)

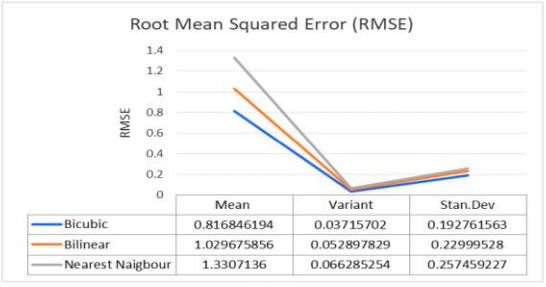

	Mean	Variant	Stan.Dev
Bicubic	0.816846194	0.03715702	0.192761563
Bilinear	1.029675856	0.052897829	0.22999528
Nearest Naigbour	1.3307136	0.066285254	0.257459227

(b)

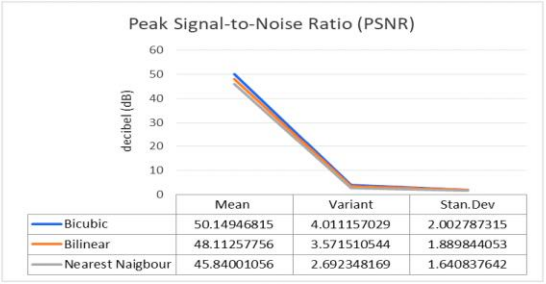

	Mean	Variant	Stan.Dev
Bicubic	50.14946815	4.011157029	2.002787315
Bilinear	48.11257756	3.571510544	1.889844053
Nearest Naigbour	45.84001056	2.692348169	1.640837642

(c)

Figure 4. Graph of (a) MSE, (b) RMSE and (c) PSNR value

Fig. 4 shows a graph of the average of Mean Square Error (MSE), Root Mean Squared Error (RMSE), and Peak Signal-to-Noise Ratio (PSNR) of 20 sample images. The blue line is the value of the resizing process using the bicubic interpolation method, the orange color line is the value of the resizing result using the bilinear interpolation method, and the green color line is the value of the resizing result using the nearest neighbor method. The bicubic interpolation method has the smallest error level for image resizing compared to the other two methods, bilinear interpolation, and nearest-neighbor interpolation.

The second process detected the location of the optic disk Fig. 5 shows sample images after optic disk detection; we select the potential OD regions by computing the area of the retinal image.

Figure 5. Optic Disk detected

From 100 samples image, 89 images correctly detected the location of OD and precisely determined the area of ROI, while 11 images failed to determine the location of OD and determined the area of ROI, this is because there is an area in the retina whose brightness level exceeds the average brightness level of OD.

The third process computed the region of interest (ROI) area in the retinal image, The ROI area is determined based on the optical disk detection point then cropping in the area around the optical disk with a size of 1.5 the diameter of the optical disk. Fig. 6 shows the region of interest selected.

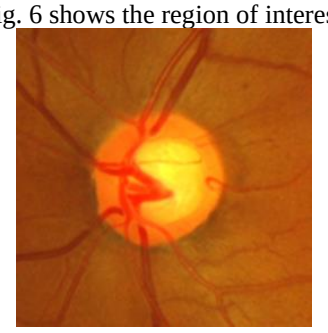

Figure 6. Region of Interest area selected

The fourth step detected the edge of the vessel, extracted the arterial and venous profiles, and noise reduction to eliminate the wrong detection of the edge of the vessels. Fig. 7 shows the results of the edge detection processes.

The fifth process measured the diameter ratio of arteries and veins (AVR). AVR measurement begins by categorizing arteries and veins on all vessel segments. Then each vessel segment is determined to be the smallest and largest diameter from the list of diameter measurements; this applies to all vessel segments of the arterial and venous categories. The last is to determine the smallest and largest diameter of the entire vessel segment for arterial and venous categories to obtain the AVR value.

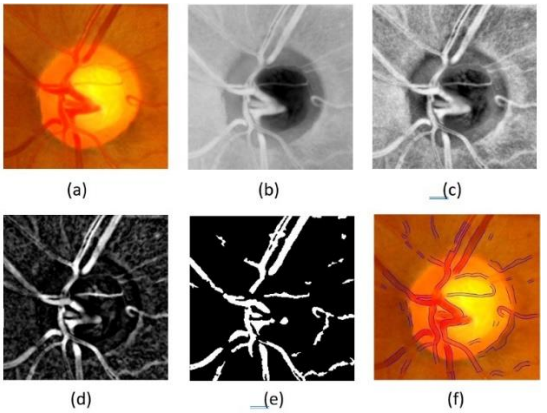

Figure 7. (a) Original Image, (b) Green channel, (c) Adaptive histogram equalization, (d) Morphology, (e) Segmented, (f) Vessel edge

Fig. 8 shows a graph of the average of AVR value, The horizontal axis is the average value of CRAE, CRVE, and AVR from 89 sample images, and the vertical axis is the vessel diameter value calculated and artery-vein ratio.

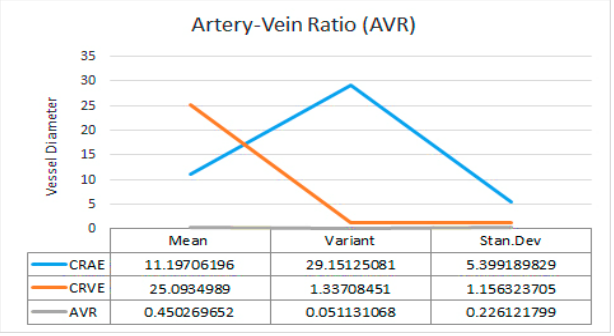

	Mean	Variant	Stan.Dev
CRAE	11.19706196	29.15125081	5.399189829
CRVE	25.0934989	1.33708451	1.156323705
AVR	0.450269652	0.051131068	0.226121799

Figure 8. Graph of AVR Value According to the Image Samples

Fig. 9 shows the hypertensive retinopathy stage categorized based on the AVR value. The blue bar is the result of classification based on the new classification proposed of hypertension retinopathy, while the orange bar is the result of the retinopathy classification from Messidor.

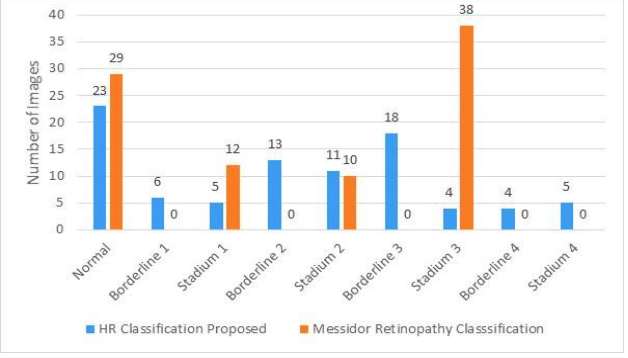

Figure 9. The classification Result

In Fig. 9, the results of the proposed new classification produce smoother grades into nine classes compared to the Messidor classification of only four classes, namely grade 0 to grade 3. The results of our testing method for classification into 4 classes were compared with the Messidor label class, from a total of 89 sample images 87 images were classified to the correct class with an accuracy rate of 97.76%. Table 1 shows a comparison of the performance of retinopathy classifications between the proposed methods and those of other previous researchers.

Table 1. Performance Comparison

Author	Dataset (Images)	Accuracy (%)
Ortiz et al. [16].	Local (30)	57
Agurto et al. [17].	Local (72)	80
Manikis et al. [18]	DRIVE	93.71
	STARE	93.18
Khitran et al. [19]	VICAVR	96.5
	DRIVE	98
Proposed Method	**MESSIDOR**	**97.76**

IV. CONCLUSION

In this paper, we discuss a new technique for determining the stage of hypertension retinopathy based on the ratio of arterial-venous diameter (AVR), which can measure the diameter of arteries and veins. The process begins with resizing to 256 x 256 pixels, using bicubic interpolation with better results. Our method applies software to measure the diameter of blood vessels of the retina. The determination of arteries and veins is determined by the semi-automatic method to obtain the AVR value.

The results obtained, with our system, can be used as a tool for determining the stage of hypertensive retinopathy based on AVR with an accuracy rate of 97.76%. Furthermore, this method can be developed by adding different parameters such as narrowing of focus, nickel arteriovenous, and other features, to get more accurate results.

References

[1] National heart lung and blood institute, *The Morbidity and Mortality: Chartbook on Cardiovascular, Lung and Blood Diseases*, US Department of Health and Human Services, National Institute of Health, Bethesda, MD, 1998.

[2] T. Y. Wong, R. Klein, B. E. K. Klein, and J. M. Tielsch et al., "Retinal microvascular abnormalities, and their relation to hypertension, cardiovascular diseases, and mortality," *Survey Ophthalmol*., vol. 46, pp. 59–80, 2001. https://doi.org/10.1016/S0039-6257(01)00234-X.

[3] L. D. Hubbard and R. J. Brothers et al., "Methods for evaluation of retinal microvascular abnormalities associated with hypertension/sclerosis in the atherosclerosis risk in communities studies," *Ophthalmology*, vol. 106, pp. 2269–2280, 1999. https://doi.org/10.1016/S0161-6420(99)90525-0.

[4] T. Y.Wong, L. D. Hubbard, and R. Klein et al., "Retinal microvascular abnormalities and blood pressure in older people: the cardiovascular health study," *Br. J. Ophthalmol*., vol. 82, pp. 1007–1013, 2002. https://doi.org/10.1136/bjo.86.9.1007.

[5] A. Hoover, V. Kouznetsova, and M. Goldbaum, "Locating blood vessels in retinal images by piecewise threshold probing of a matched filter response," *IEEE Trans. Medical Image.*, vol. 19, issue 3, pp. 203–210, Mar. 2000. https://doi.org/10.1109/42.845178.

[6] Y. A. Tolias and S. M. Panas, "A fuzzy vessel tracking algorithm for retinal images based on fuzzy clustering," *IEEE Trans. Medical Image*., vol. 17, issue 2, pp. 263–273, 1998. https://doi.org/10.1109/42.700738.

[7] M. Lalonde, L. Gagnon, and M. C. Boucher, "Non-recursive paired tracking for vessel extraction from retinal images," *Proceedings of the International Conference on Vision Interface*, 2000, pp. 61–68.

[8] R. M. Haralick, S. R. Sternberg, and X. Zhuang, "Image analysis using mathematical morphology," *IEEE Trans. Pattern Analysis Mach. Intell*., vol. PAMI-9, pp. 532–550, 1987. https://doi.org/10.1109/TPAMI.1987.4767941.

[9] T. McInerney and D. Terzopoulos, "Deformable models in medical image analysis: a survey," *Medical Image Analysis*., vol. 1, issue 2, pp. 91–108, 1996. https://doi.org/10.1016/S1361-8415(96)80007-7.

[10] M. Goldbaum, S. Moezzi, A. Taylor, and S. Chatterjee et al., "Automated diagnosis and image understanding with object extraction, object classification, and inferencing in retinal images," *Proceedings of the IEEE International Conference Image Processing*, vol. 3, 1996, pp. 695–698.

[11] O. Chutatape, Z. Liu, and S. M. Krishnan, "Retinal blood vessel detection and tracking by matched Gaussian and Kalman filters," *Proceedings of the 20th Annual Conference. IEEE Engineering. Med. Biol. Soc*., 1998, pp. 3144–3148.

[12] I. Liu and Y. Sun, "Recursive tracking of vascular networks in angiograms based on the detection-deletion scheme," *IEEE Trans. Medical Image*., vol. 12, issue 2, pp. 334–341, 1993. https://doi.org/10.1109/42.232264.

[13] P. Jasiobedzki, C. J. Taylor, and J. N. H. Brunt, "Automated analysis of retinal images," *Image Vision Computing*, vol. 11, issue 3, pp. 139–144, 1993. https://doi.org/10.1016/0262-8856(93)90052-I.

[14] G. Luo, O. Chutatape, and S. M. Krishnan, "Detection and measurement of retinal vessels in fundus images using amplitude modified second-order Gaussian filter," *IEEE Tran. Biomed. Eng*., vol. 49, issue 2, pp. 168–172, 2002. https://doi.org/10.1109/10.979356.

[15] W. H. Spencer, "Ophthalmic Pathology: An Atlas and Text-book." *Philadelphia*, PA: Saunders, 1996.

[16] D. Ortíz, M. Cubides, A. Suárez, M. Zequera, J. Quiroga, J. Gómez, & N. Arroyo, "Support system for the preventive diagnosis of hypertensive retinopathy," *Proceedings of the 2010 Annual International Conference of the IEEE Engineering in Medicine and Biology*, 2010, pp. 5649-5652. https://doi.org/10.1109/IEMBS.2010.5628047.

[17] C. Agurto, V. Joshi, S. Nemeth, P. Soliz, & S. Barriga, "Detection of hypertensive retinopathy using vessel measurements and textural features," *Proceedings of the 2014 36th Annual International Conference of the IEEE Engineering in Medicine and Biology Society*, 2014, pp. 5406-5409. https://doi.org/10.1109/EMBC.2014.6944848.

[18] G. C. Manikis, V. Sakkalis, X. Zabulis, P. Karamaounas, A. Triantafyllou, S. Douma, & K. Marias, "An image analysis framework for the early assessment of hypertensive retinopathy signs," Proceedings of the 2011 IEEE E-Health and Bioengineering Conference (EHB), 2011, pp. 1-6.

[19] S. Khitran, M. U. Akram, A. Usman, & U. Yasin, "Automated system for the detection of hypertensive retinopathy," *Proceedings of the 2014 4th IEEE International Conference on Image Processing Theory, Tools and Applications (IPTA)*, 2014, pp. 1-6. https://doi.org/10.1109/IPTA.2014.7001984.

[20] L. D. Hubbard *et al.*, "Methods for evaluation of retinal microvascular abnormalities associated with hypertension/sclerosis in the atherosclerosis risk in communities study," *Ophthalmology*, vol. 106, pp. 2269–2280, 2013. https://doi.org/10.1016/S0161-6420(99)90525-0.

[21] L. Downie, S. Rogers, and P. P. Connell, "Hypertensive retinopathy: Comparing the Keith-Wagener-Barker to a simplified classification?," *Journal of Hypertension*, vol. 31, issue 5, pp. 960-965, 2013. https://doi.org/10.1097/HJH.0b013e32835efea3.

[22] Messidor, *Methods for Evaluating Segmentation and Indexing techniques Dedicated to Retinal Ophthalmology*. [Online]. Available at: http://www.adcis.net/en/Download-Third-Party/Messidor.html.

[23] J. Titus, M. T. S. CSE, and S. Geroge, "A comparison study on different interpolation methods based on satellite images," *International Journal of Engineering Research & Technology*. vol. 2. Issue. 6, pp. 82–85. 2013.

[24] S. Yuan, M. Abe, A. Taguchi, and M. Kawamata, "High accuracy bicubic interpolation using image local features," *IEICE Transactions on Fundamentals of Electronics, Communications, and Computer Sciences*, vol. 90, issue 8, pp. 1611–1615, 2007. https://doi.org/10.1093/ietfec/e90-a.8.1611.

[25] H.S. Prashanth, H.L. Shashidhara, & K.N. Balasubramanya Murthy, M. "Image scaling comparison using universal image quality index," *Proceedings of the 2009 International Conference on Advances in Computing, Control, and Telecommunication Technologies*, 2009, pp. 859-863. https://doi.org/10.1109/ACT.2009.218.

[26] A. Bhuiyan, R. Kawasaki, and E. Lamoureux, "Retinal artery – vein caliber grading using color fundus," *Computer Methods and Programs in Biomedicine*, vol. 111, issue 1, pp. 104–114, 2013. https://doi.org/10.1016/j.cmpb.2013.02.004.

[27] J. Canny, "A computational approach to edge detection," *IEEE Transactions on Pattern Analysis and Machine Intelligence*, vol. 8, issue 6, pp 679–698, 1986. https://doi.org/10.1109/TPAMI.1986.4767851.

[28] R. C. Gonzalez, R. Woods, *Digital Image Processing*, 3rd ed, Pearson Prentice Hall, 2008.

BAMBANG KRISMONO TRIWIJOYO *is a doctoral candidate in the doctoral program in Computer Science, Bina Nusantara University, Jakarta – Indonesia. He obtained a bachelor's degree, majoring in Informatics Engineering, STIKI Malang – Indonesia in 1992. He continued his master's degree in Informatics Engineering from the Sepuluh November Institute of Technology (ITS), Surabaya – Indonesia. He obtained his Masters's in Computer Engineering in 2003. The author is an assistant professor at Bumigora University until now. Starting in 2016 he continued his doctoral studies in the doctoral program in Computer Science, Bina Nusantara University, Jakarta – Indonesia. He is a member of Indonesian pattern recognition (INAPR), Indonesian Informatics Expert Association (IAII). His research interests are in image processing, pattern recognition, artificial intelligence especially in the medical field.*

Boy Subirosa Sabarguna *was born in Majaleng-ka, West Java, in 1958. The author completed his medical education at the Faculty of Medicine, University of Indonesia (FK UI) in 1984, completed his education in Hospital Administration (MARS) at the University of Indonesia (UI) in 1991, and graduated from the Doctor of Postgraduate Program at Gajah Mada University in 2001. The author is currently active as a lecturer at the Public medical science, University of Indonesia (IKK-FKUI), TBM-PPSUI, and as a Hospital Management Consultant. The author is also active in writing books in the context of developing, improving, and disseminating knowledge. Currently, the books he has written have reached 68 titles, mainly in the field of hospital management, and made software with a team of 8 IPRs in the form of a Decision Support System.*

WIDODO BUDIHARTO *is a professor of Artificial Intelligence at the School of Computer Science, Bina Nusantara University, Jakarta – Indonesia. He obtained his bachelor's degree, major in physics from the University of Indonesia (UI), Jakarta – Indonesia in 2000. He continued his study in information technology major at STT Benarif, Jakarta – Indonesia, and obtained his Master in Information Technology in 2003. He obtained his Ph.D. in Electrical Engineering from the Institute of Technology Sepuluh Nopember (ITS), Surabaya – Indonesia in 2012. He took his Ph.D. Sandwich Program in Robotics and Artificial Intelligence at Hosei University – Japan and Postdoc in Robotics and Artificial Intelligence at Hosei University – Japan, and Erasmus Mundus Scholar EU Univer-site de Bourgogne – French Indonesia Consortium (FICEM) – French in 2017, in 2016, in 2008, respectively. His research interest is in intelligence systems, data science, robot vision, and computational intelligence.*

EDI ABDURACHMAN *obtained the Professorship of Statistics in 2008 and was inaugurated at Bina Nusantara University in 2009. He graduated from Iowa State University, Ames, the USA with a doctoral degree in statistics in 1986. The Master of Science conferred from the same University in a statistics survey in 1983. He also earned a Master of Science degree in applied statistics from Bogor Agricultural University. He obtained the Agriculture Engineering Degree (Ir) from IPB (cum laude) in 1978. Since 1986, He has served as a lecturer at Bina Nusantara University, Jakarta. His teaching expertise included Linear Algebra, Discrete Mathematics, Mathematical Statistics, Business Statistics, Operations research, Information Systems, Research Methods, and others. He has professional experience as a statistical consultant for various companies in Indonesia and attends varied national and international statistical courses. He was invited as a speaker at international conferences and various seminars, e.g., Statistics and data Utilization for Agricultural Policy of Indonesia in Myanmar and the Economics Modeling for Agricultural Sector. The case of Predicting some Agricultural Strategic Commodities; The Office of Agricultural Economics (OAE) and JICA ASEAD, in Bangkok, Thailand. He also published research in statistics. He is also a member of the American Statistics Association, the International Association of Engineers (IAENG), and the honorary member of the MU SIMA RHO Society.*